Deep-Sea Research, Vol. 36, No. 1, pp. 39–53, 1989.
Printed in Great Britain.

0198-0149/89 $3.00 + 0.00

On the size of the Antarctic Circumpolar Current

GREGORY C. JOHNSON* and HARRY L. BRYDEN†

(*Received* 7 *March* 1988; *in revised form* 17 *August* 1988; *accepted* 19 *August* 1988)

Abstract—A model predicted transport of the Antarctic Circumpolar Current (ACC) through Drake Passage compares favorably with measured transport through the passage. The model incorporates the width of the ACC, the strong eddy presence in the region, and the deep penetration of an unstable baroclinic velocity field, all of which are characteristic features of the current. The model involves a downward transfer of wind-imparted zonal momentum by eddy form drag to a depth at which it can be removed by bottom pressure drag. The eddy form drag results from a poleward transport of heat by eddies originating from the baroclinically unstable current.

INTRODUCTION

THE Antarctic circumpolar region between 56° and 62°S is the only zonally unbounded region in the world ocean. The eastward-flowing Antarctic Circumpolar Current (ACC) (Fig. 1) is constantly accelerated by the eastward wind stress applied at the ocean surface (NOWLIN and KLINCK, 1986). Since there are no continental barriers in the region, standard Sverdrup dynamics describing gyre circulations in other ocean basins are difficult to apply in this region. The Southern Ocean requires special dynamical treatment.

Lack of continental barriers nonwithstanding, initial theoretical models of the ACC were mainly adaptations of the Sverdrup dynamics relating wind stress curl to meridional transport (STOMMEL, 1957, 1962). It was realized early on, however, that such models required uncomfortably large values of eddy friction coefficients to limit the transport of the ACC to a reasonable value (MUNK and PALMEN, 1951). With the advent of numerical models of large-scale ocean circulation, various attempts at modeling the ACC yielded model transports that depended strongly on the choice of eddy friction coefficient values. GILL (1968) found that large values of vertical or horizontal friction were needed to keep his model transport to a reasonable value. (He cited a bottom friction coefficient of 10^3 cm^2 s^{-1} and a lateral friction coefficient of 10^8 cm^2 s^{-1}.)

In an early exploration of the effect of topography in a numerical model of the Southern Ocean, GILL and BRYAN (1971) ran a model in which the Southern Ocean geometry was represented by a basin zonally connected by a gap representing Drake Passage. The lower half of the gap was enclosed for one model run and the transport of

* M.I.T.–W.H.O.I. Joint Program, Woods Hole Oceanographic Institution, Woods Hole, MA 02543, U.S.A.
† Department of Physical Oceanography, Woods Hole Oceanographic Institution, Woods Hole, MA 02543, U.S.A.

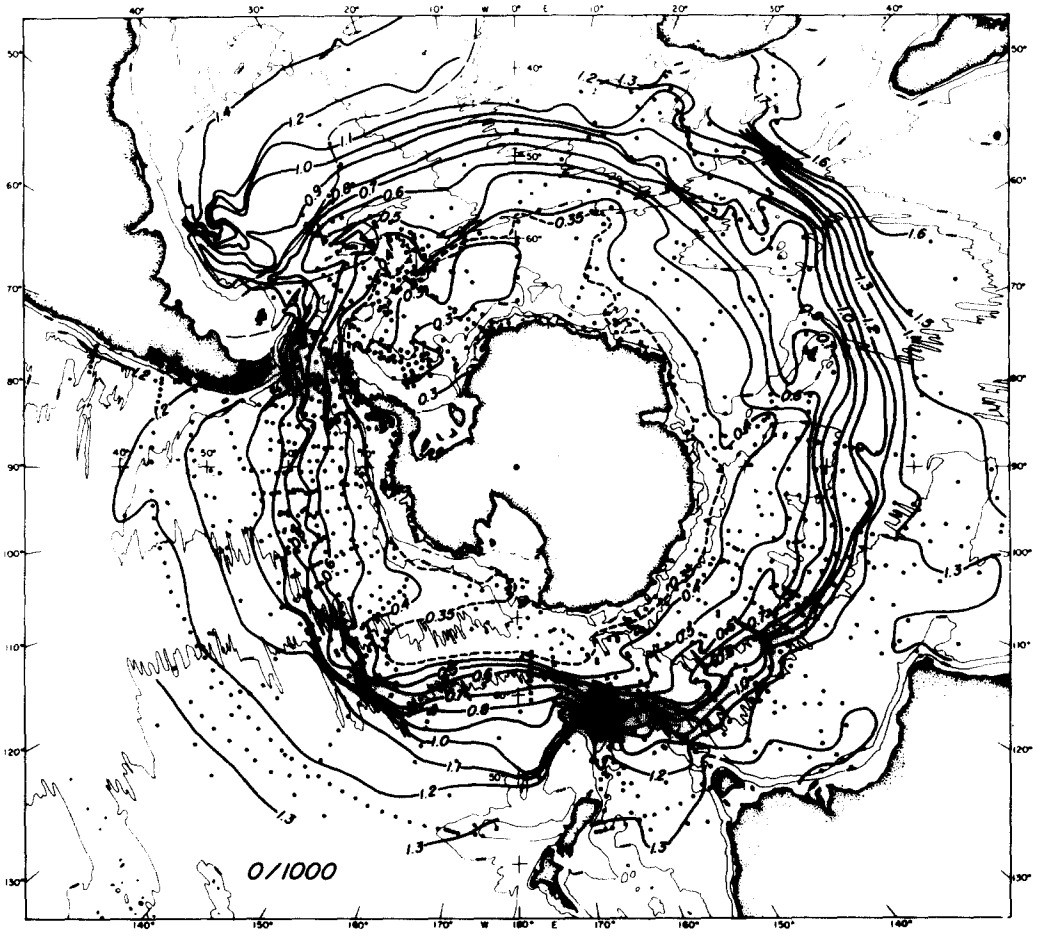

Fig. 1. 0–1000 db dynamic height field of the Southern Ocean in dynamic meters with 4000 m isobath and station locations. Figure 2 from GORDON *et al.* (1978).

the ACC increased three-fold above that in a run with the gap open to the bottom. This increase was the result of a thermal effect caused by the presence of water of differing densities on either side of the ridge. This density difference created a pressure difference across the ridge that worked with the wind to accelerate the current eastward. As discussed below in the context of work by MCWILLIAMS *et al.* (1978) the inclusion of nonlinearity and subsequent eddy formation would probably modify this result significantly.

In the early 1970s, a controversy arose over the magnitude of the transport of the ACC. Two independent attempts to determine the transport of the current through the Drake Passage by referencing geostrophic shear to short records of directly measured current gave wildly varying results. REID and NOWLIN (1971) found an eastward transport of 237 Sv, while FOSTER (1972) reported a transport of 15 Sv westward through the Drake Passage. Modeling the current was rendered meaningless, since almost any model transport was plausible in light of existing estimates. Subsequently the International

Southern Ocean Studies (ISOS) program was initiated to measure the transport through Drake Passage.

NOWLIN and KLINCK (1986) have reviewed observational and theoretical progress in understanding the transport, structure and dynamics of the ACC over the decade of the ISOS program. They report a mean transport through Drake Passage of 134 Sv with an uncertainty of 10% and a time variability estimated at 20%. Most variability is seen in the barotropic field and not in the baroclinic shear. Since no existing theoretical or numerical model of the ACC adequately predicts this transport, new models are needed to examine the factors determining the size of the ACC.

Several features of the ACC have been observed in the past decade or so. First, the current is not a narrow jet or boundary current with a width equal to the internal Rossby radius of deformation. While NOWLIN and KLINCK (1986) emphasize that three narrow frontal regions of scale two to three times the Rossby radius carry most of the transport, the current does extend completely across Drake Passage (Fig. 2). Secondly, the ACC penetrates down to the bottom of the water column, with substantial meridional density

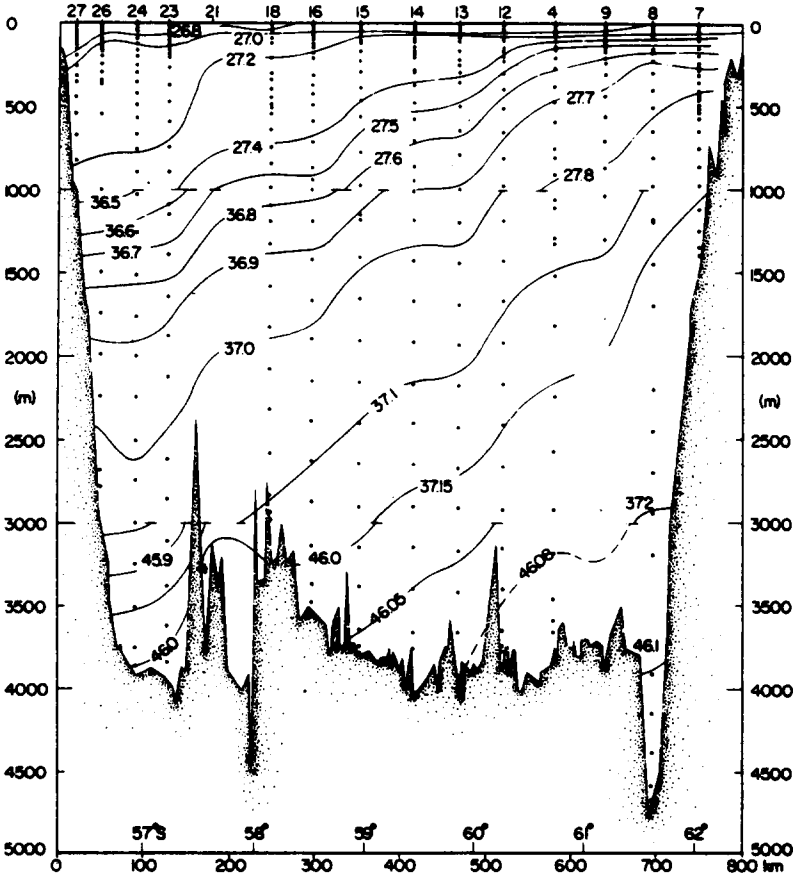

Fig. 2. Section of variability referenced density parameter σ across Drake Passage calculated from *Melville* Section II FDRAKE 75 data. Figure 4 from NOWLIN *et al.* (1977).

gradients at depth (Fig. 2). Thirdly, there is energetic eddy activity associated with the Circumpolar Current (BRYDEN, 1983). The eddies transport a significant amount of heat downgradient, or poleward, through a baroclinic instability process in which the eddies grow by converting available potential energy contained in the large-scale baroclinic field to eddy kinetic and potential energy (BRYDEN, 1979a).

With regard to the prominence of eddies in the region indicated by early ISOS results, MCWILLIAMS *et al.* (1978) developed an eddy resolving numerical model of the ACC. They constructed a two-layer quasi-geostrophic model of a zonally connected region and ran it with various channel geometries and wind forcing functions. One run included a Gaussian bump rising to block an eighth of the lower layer depth in the gap which represented Drake Passage. The bump simulated the Scotian Arc, which rises to 2000 m depth just east of Drake Passage and constitutes the greatest topographic obstruction to the ACC. Unfortunately, the quasi-geostrophic dynamics chosen greatly restricted the height of the topographic rise used in the model, but some interesting results did emerge from the runs. In all model runs eddies played a significant role in transporting eastward momentum from the upper layer down to the lower layer, where most of the momentum imparted by wind stress was dissipated by bottom friction or by topographic pressure drag. Realistic bottom friction was too weak to dissipate enough momentum to keep transport values below 400–600 Sv. Only in the run with the topographic rise did bottom pressure drag or mountain drag provide a mechanism for removing eastward momentum strong enough to limit model transport to 100 Sv.

The goal of this paper is to present a simple model of the dynamics of the ACC that predicts a transport independent of friction coefficients. In the process of making this transport prediction, attempts are made at explaining why the current is as wide as it is, why baroclinic density gradients penetrate to great depth, and how the eddies shape the baroclinic density field and match the downward momentum transfer with the wind stress imparted momentum thus determining the transport of the ACC.

THE CIRCUMPOLAR ZONAL MOMENTUM BALANCE

Many models have emphasized the vorticity dynamics of the ACC (STOMMEL, 1957, 1962), but the zonal nature of the flow indicates a need to understand first the zonally and vertically integrated eastward momentum balance for the steady circumpolar circulation. This balance can be written

$$\oint dx \left[\frac{\partial}{\partial x} \int_{z=-H}^{0} dz(uu) + \frac{\partial}{\partial y} \int_{z=-H}^{0} dz(uv) = \int_{0}^{-H} dz \left(fv - \frac{1}{\rho_0} \frac{\partial p}{\partial x} + \frac{1}{\rho_0} \frac{\partial \tau^x}{\partial z} \right) \right], \tag{1}$$

where (u, v, w) are the velocities in the (x = east, y = north, z = upward) directions, f is the Coriolis parameter, ρ_0 is the density of seawater, and τ^x is the eastward stress component. Equation (1) owes its unconventional form to manipulations involving the chain rule, the continuity equation, and the imposition of a rigid lid at $z = 0$. Since the meridional transport must vanish over the area of integration the Coriolis force term, fv, is zero. For a zonally connected ocean the term $\int_{z=-H}^{0} dz(uu)$ is also zero. Thus the integrated eastward momentum balance reduces to

$$\oint dx \left[\frac{\partial}{\partial y} \int_{z=-H}^{0} dz(uv) + \int_{z=-H}^{0} dz \frac{1}{\rho_0} \frac{\partial p}{\partial x} \right] = \frac{1}{\rho_0} \oint dx \tau^x \Big]_{bottom}^{surface} \tag{2}$$

in the circumpolar region.

For a flat-bottomed circumpolar region $\oint dx \int_{z=-H}^{0} dz\ 1/\rho_0\ \partial p/\partial x = 0$ and the wind stress at the sea surface (of order 2 dyn cm^{-2}, see NOWLIN and KLINCK, 1986) must be balanced either by the meridional divergence of eastward momentum flux $\partial/\partial y \int dz(uv)$, or bottom stress. GILL (1968) argued convincingly that bottom stress is unlikely to be as large as wind stress. He calculated that a meridional flux of zonal momentum $\overline{u'v'}$ of order 100 $cm^2\ s^{-2}$ on the northern and southern edges of the ACC would balance the eastward stress. These meridional fluxes of zonal momentum are equivalent to the large lateral viscosity coefficients that many models require.

Recent analyses indicate that observed meridional momentum fluxes are not nearly large enough to balance the wind stress and give a reasonable transport value. BRYDEN and HEATH (1985) observed a statistically significant northward eddy flux of eastward momentum on the northern edge of the ACC downstream of the Macquarie Ridge where this momentum flux was anticipated to be large. Even if it were typical of the entire circumpolar zone, which was considered unlikely, the measured eddy momentum flux was smaller by a factor of four than that required by GILL (1968). Bryden and Heath also estimated the standing eddy momentum flux due to large-scale variations in the circumpolar circulation from historical data compiled by GORDON *et al.* (1982) and found it to be two orders of magnitude smaller than that required to balance the wind stress. Finally, PIOLA *et al.* (1987) determined the eddy momentum flux at the surface from the large-scale FGGE drifter deployment during 1979 and found it to be a factor of three smaller than that required to balance the wind stress, even in the unlikely instance that the surface values were typical of depth-averaged ones. Thus the meridional divergence of the meridional flux of eastward momentum does not appear to be large enough to balance the eastward wind stress in the circumpolar region.

The alternative balancing mechanism for the eastward wind stress is bottom form drag, or mountain drag, in which high pressure is found on the upstream side of submarine ridges or seamounts (Fig. 3). MUNK and PALMEN (1951) first suggested mountain drag as

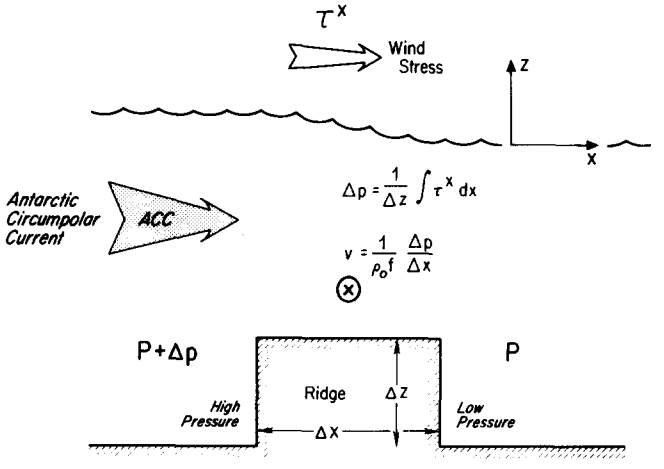

Fig. 3. Schematic presentation of bottom form drag or mountain drag. Wind stress imparted eastward momentum in the water column is removed by the pressure difference across the ridge. Note that geostrophic balance $\rho_0 fv = \partial p/\partial x$ demands an equatorward flow (symbolized by ⊗) along the ridge, evidence of which may be seen in Fig. 1.

the most likely counterbalance to the eastward wind stress in the circumpolar region. They estimated a 4 dyn cm pressure difference across each of the four major ridges (the Scotian Arc, the Kerguelan Plateau, the Macquarie Ridge and the South Pacific Ridge) to be sufficient to balance the zonal wind stress. A steady-state balance requires that the pressure difference Δp across the ridge must be directly related to the wind stress by $\Delta p = 1/\Delta z \int \tau^x dx$, where Δz is the height of the ridge above the flat bottom (Fig. 3).

If the zonal wind stress decreases to zero over a surface Ekman layer and the deep mid-ocean zonal pressure gradient is in geostrophic balance, then the equatorial Ekman transport in the surface waters is balanced by an equivalent poleward transport of deep water. The conversion of denser deep water into lighter surface water around the Antarctic, as is necessary to close such a vertical-meridional circulation, goes against conventional air–sea-ice exchange considerations that argue for large buoyancy loss over the Southern Ocean (GORDON and OWENS, 1987).

Alternatively, as MUNK and PALMEN (1951) suggested, the eastward wind stress may be transmitted downward undiminished to the deep ocean where it is balanced directly by bottom form drag. RHINES and HOLLAND (1979) discussed such a transmission of zonal momentum downward by eddies produced as a result of instability in a zonal current. Such downward momentum transfer would imply the absence of a surface Ekman layer in the circumpolar region.

Consider a two-layer circumpolar ocean (Fig. 4) with variations η', in the free surface, and ζ', in the interface height about their mean values. The interfacial form drag between the layers can be estimated to be $\oint p' \, \partial\zeta'/\partial x \, dx$, analogous to mountain drag if the lower

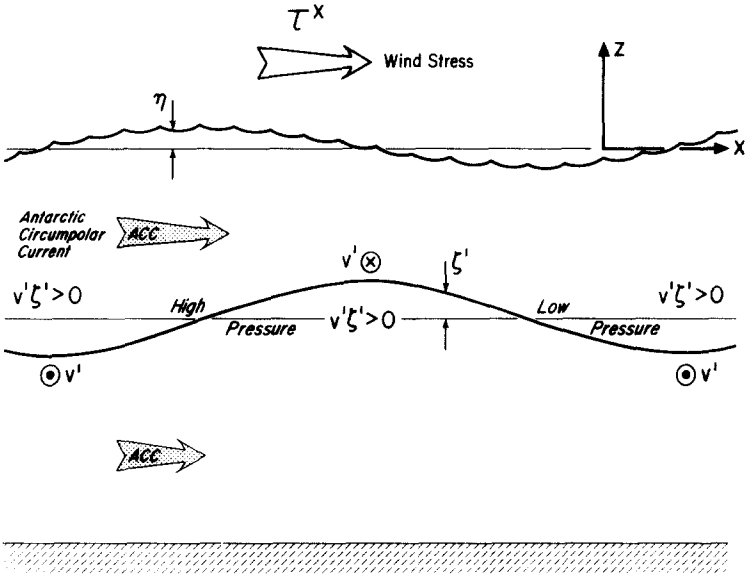

Fig. 4. Schematic presentation of interfacial form drag. Correlations of perturbations in the interface height, ζ', and the meridional velocity, V' (⊙ indicating poleward flow and ⊗ indicating equatorward flow), which are related to pressure perturbations by geostrophy, allow the upper layer to exert an eastward force on the lower layer and the lower layer to exert a westward force on the upper layer; thus effecting a downward flux of zonal momentum.

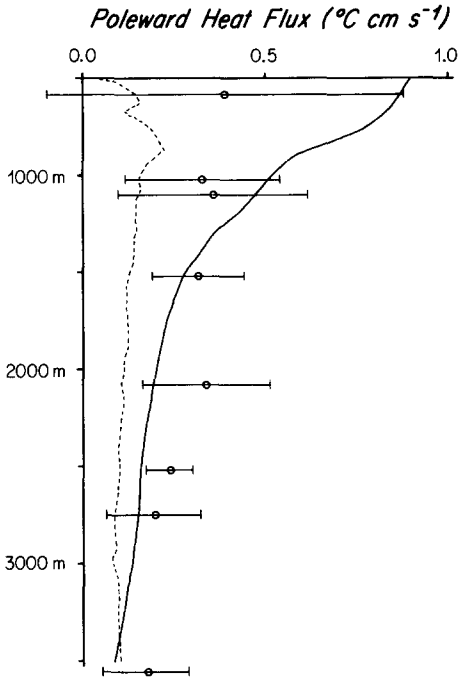

Fig. 5. Measured eddy heat flux in central Drake Passage (discrete points with standard error bars) plotted with eddy heat flux predicted from a momentum flux balance argument (equation (4), dashed line) and a large-scale baroclinic field parameterization (equation (5), solid line).

Table 1. *Eddy heat flux and downward momentum flux for current meter records in central Drake Passage. Data used were taken in Drake Passage during the ISOS program. Current meter data used to calculate eddy heat flux values is taken from the* 1977 *central Drake Passage Cluster Array at* 59°S, 64°W (BRYDEN, 1979b), *and moorings* 8 (59°S, 64°30′W) *and* 10 (60°S, 63°W) *from the FDRAKE* 75 *mooring array. Calculation of* $\overline{\theta}_z$ *was performed using an arithmetic mean of hydrographic/STD stations* 13, 14, 15, 33 *and* 42 *taken near the moorings by the R.V.* Melville *during FDRAKE* 75. *Values of* $\rho_0 = 1.03$ g cm^{-3} *and* $f = -1.25 \times 10^{-4}$ s^{-1} (*appropriate for* 59°S) *were used. See* NOWLIN et al. (1977) *Fig.* 1, *for locations of R.V.* Melville *stations and moorings* 8 *and* 10

Depth (m)	Eddy heat flux $\overline{V'T'}$ (°C cm s^{-1})	Vertical temperature gradient $\overline{\theta}_z$ ($\times 10^{-4}$ °C cm^{-1})	Downward momentum flux $\rho_0 f \overline{V'T'}/\overline{\theta}_z$ (dyn cm^{-2})
580*	–0.39	0.066	7.6
1020†	–0.33	0.056	7.6
1100*	–0.36	0.056	8.3
1520†	–0.32§	0.079	5.2
2080*	–0.34§	0.074	5.9
2520†	–0.24§	0.079	3.9
2750‡	–0.20	0.074	3.5
3560*	–0.18	0.054	4.3

* 1977 Drake Passage Cluster Array Moorings.
† FDRAKE 75 mooring 10.
‡ FDRAKE 75 mooring 8.
§ Significantly different from zero at the 95% confidence level.

layer were a rigid ocean bottom. Note that as opposed to mountain drag, interfacial form drag is not a depth-integrated zonal force. The zonally averaged pressure gradient remains zero for the circumpolar region above submarine ridges. Interfacial form drag causes a vertical flux of zonal momentum from the upper layer to the lower layer, leaving the depth-integrated zonal momentum balance unchanged. An equivalent expression for the interfacial form drag $-\oint \zeta' \, \partial p'/\partial x \, dx$ can be obtained simply by integrating by parts over the zonally connected circumpolar region. The two-layer concept can be extended to the case of continuous stratification where $\zeta' = -T'/\overline{\theta}_z$, with T' the temperature perturbation about its average value and $\overline{\theta}_z$ the vertical gradient of potential temperature. Considering geostrophic motions where $1/\rho_0 \, \partial p'/\partial x = fv'$ results in the final expression for the form drag

$$\oint p' \frac{\partial \zeta'}{\partial x} \, dx = -\oint \zeta' \frac{\partial p'}{\partial x} \, dx = \oint f \frac{\overline{v'T'}}{\overline{\theta}_z} \, dx. \tag{3}$$

This form drag is a vertical flux of eastward momentum which is proportional to the meridional eddy heat flux: poleward heat flux corresponds to downward flux of eastward momentum. Form drag is equivalent to the vertical component of Eliassen–Palm flux and it is only the vertical divergence of this flux which accelerates zonal currents (HOSKINS, 1983).

THE MODEL

The following prediction of the transport of the ACC is based on two assumptions. First, eddies are assumed to transmit eastward wind stress downward into the deep water where bottom form drag can balance this stress. Thus, the downward eddy flux of eastward momentum is taken equal to the wind stress throughout the water column;

$$\rho_0 f \frac{\overline{v'T'}}{\overline{\theta}_z} = \tau^x. \tag{4}$$

We can test this relation using ISOS current meter and central Drake Passage hydrographic data to compute eddy heat flux. Table 1 gives values of the left-hand-side of equation (4) to be compared to a value of about 2 dyn cm^{-2} for eastward wind stress over the ACC (NOWLIN and KLINCK, 1986). The eddy heat fluxes have the correct sign to transmit the wind-imparted zonal momentum downward. The magnitudes indicated are larger than that of the wind stress over the current, but this difference is not disturbing in light of the uncertainty in the values calculated. (See Table 1 and Fig. 5 for error estimates.) Other contributions toward this discrepancy could include spacial variation of eddy heat flux around the ACC and the role of meridional eddy fluxes of zonal momentum within the current. These topics are touched upon in the Discussion.

The second assumption is that the eddy fluxes result primarily from a baroclinic instability process in which eddies grow by tapping available potential energy associated with the large-scale baroclinic field. For such a process, GREEN (1970) and STONE (1972, 1974) suggested that the down-gradient eddy heat flux $\overline{v'T'}$ could be parameterized in

terms of the time average baroclinic fields:

$$V' \propto H\overline{U_z}$$

$$T' \propto \pi R_0 \overline{T_y}$$

so

$$\overline{V'T'} = CH\pi R_0 \overline{U_z}\,\overline{T_y}, \tag{5}$$

where H is the water depth, $R_0 = \int_{z=-H}^{z=0} N(z)\mathrm{d}z/\pi f_0$ is the Rossby radius of deformation, $\overline{U_z}$ is the vertical shear of the time average zonal velocity field, $\overline{T_y}$ the large-scale meridional temperature gradient, and C is the correlation coefficient between velocity and temperature fluctuations. The parameterization is based on the idea that temperature fluctuations are the result of lateral displacement of the mean baroclinic temperature field over distances of order a Rossby radius of deformation and that velocity variations are typically of the same size as the time-averaged velocities near the strong current. STONE (1974) actually predicted a value of $C = 0.144$ from an analytical study. Since the time-averaged vertical shear and the meridional temperature gradient are related by the thermal wind balance, $\rho_0 f\overline{U_z} = g\alpha\overline{T_y}$, where g is gravity and $\alpha = -\mathrm{d}\rho/\mathrm{d}T$, equation (5) can be rearranged to argue that eddy heat flux is proportional to the square of the vertical shear of the time-averaged zonal current.

$$\overline{V'T'} = CH\pi R_0 \frac{\rho_0 f_0}{g\alpha} \overline{U_z^2}. \tag{6}$$

This parameterization is tested with ISOS current meter and hydrographic data in the Drake Passage by calculating a value for C from the data. Results are displayed in Table 2. Comparison of results to Stone's correlation coefficient value of $C = 0.144$ shows observation and theory agree to better than an order of magnitude.

Figure 5 graphically illustrates tests of equations (4) and (5) by predicting heat fluxes with each and comparing to measured heat flux values. The prediction with equation (4) is made using a $\tau_x = 2$ dyn cm^{-2}, and $f = -1.25 \times 10^{-4}$ s^{-1} (a value for 59°S) and a $\overline{\theta}_z$

Table 2. Test of Stone's eddy heat flux parameterization for Drake Passage current meter and hydrographic data. The source for eddy heat flux values is documented in Table 1. *A value of* 3500 m *was chosen for the depth of the passage* H. *The Rossby radius* R_0 *was calculated using an* N^2 *constructed from an arithmetic mean of hydrographic/STD stations* 8, 9, 4, 12, 14, 15, 16, 18, 20, 23 *and* 24 *taken by R.V.* Melville *and spanning the passage (see Table* 1 *for details). Calculations of* $\overline{U}_z$ *and* $\overline{T}_y$ *were performed with deep end stations* 8 *and* 24

Depth (m)	Eddy heat flux $\overline{V'T'}$ (°C cm s^{-1})	Large-scale scaled baroclinic shear fields $H\pi R_0\overline{U_z}\,\overline{T_y}$(°C cm s^{-1})	Correlation coefficient $C = \overline{V'T'}/H\pi R_0\overline{U_z}\,\overline{T_y}$
580*	–0.39	6.35	0.06
1020†	–0.33	3.73	0.09
1100*	–0.36	3.39	0.11
1520†	–0.32§	2.04	0.16
2080*	–0.34§	1.37	0.25
2520†	–0.24§	1.12	0.21
2750‡	–0.20	1.09	0.18
3560*	–0.18	0.56	0.32

* 1977 Drake Passage Cluster Array Moorings.
† FDRAKE 75 mooring 10.
‡ FDRAKE 75 mooring 8.
§ Significantly different from zero at the 95% confidence level.

from the central Drake Passage station average described in Table 1. The $\overline{V'T'}$ prediction with equation (5) is made with $C = 0.144$, $H = 3500$ m, the Rossby radius of deformation calculated from the full Drake Passage average described in Table 2, with $\overline{U_z}$ and $\overline{T_y}$ calculated from the end stations. Measured $\overline{V'T'}$ values are those in Tables 1 and 2. Both predictions fall nearly within a standard error of the measured heat flux, and are of the correct sign.

Combining the two model assumptions and eliminating the eddy heat flux, $\overline{V'T'}$, between equations (4) and (6) yields the result that the time-averaged vertical shear of the ACC is proportional to the square root of the zonal wind stress

$$\overline{U_z}(z) = \frac{N(z)}{f}\sqrt{\frac{\tau_x}{\rho_0 CH\pi R_0}}, \tag{7}$$

where $N(z) = (g/\rho_0\ \partial\bar{\rho}/\partial z)^{\frac{1}{2}}$ is the buoyancy frequency calculated from the vertical density stratification from the full Drake Passage averages. Stone's correlation coefficient of 0.144 is used in the calculations that follow, but since baroclinic shear is proportional to the square root of this number the model is not overly sensitive to the value of C. The resulting vertical variation of current shear is linearly proportional to variation in buoyancy frequency. Thus the zonal transport is proportional to the double vertical integral of the buoyancy frequency.

$$\text{transport} = \frac{W}{f_0}\left[\frac{\tau_x}{\rho_0 CHR_0\pi}\right]^{\frac{1}{2}}\int_{z=-H}^{0} dz' \int_{z'=-H}^{0} N(z'')dz'', \tag{8}$$

where W is the width of the ACC.

A mechanistic description of this model might go as follows: eastward wind stress initially accelerates the eastward current in the surface layers. As the current gets larger, it becomes baroclinically unstable and the resulting eddy heat flux transmits zonal momentum downward, deepening the eastward current. Once the current penetrates below the level of the submarine topography, bottom form drag can balance a vertical stress divergence in the deep water and hence provide the balance to the eastward wind stress. Eddy fluxes are required to transmit zonal momentum downward at a rate consonant with the eastward wind stress, and a deeply penetrating unstable baroclinic current system is needed to effect the required eddy fluxes.

The model can be tested in two ways. One way is to compare the vertical shear of zonal velocity in Drake Passage computed with the end stations and the thermal wind relation to that predicted by the model equation (7), with the Drake Passage average value of $N(z)$. Values used are $f = -1.25 \times 10^{-4}$ s^{-1} (59°S value), $\tau_x = 2$ dyn cm^{-2}, $\rho_0 = 1.03$ g cm^{-3}, $C = 0.144$, $H = 3500$ m, and $R_0 = 12.6$ km (calculated from the full Drake Passage average N^2 profile) (Fig. 6). There is reasonable agreement between the two profiles in shape and magnitude, excepting the upper few hundred meters. Seasonal variations in the upper mixed layer make comparison of theory to observation in the upper water difficult since hydrographic stations have only been made in the austral summer. The predicted current has a smaller, more uniform shear than that observed.

Halving the value of C would markedly improve the agreement of the shear profiles in Fig. 6; however, such adjustment does not seem warranted for this simple model. Velocity calculated from the Drake Passage end stations agrees well with that predicted by the model; with both velocities referenced to 3500 m (Fig. 7), the model slightly

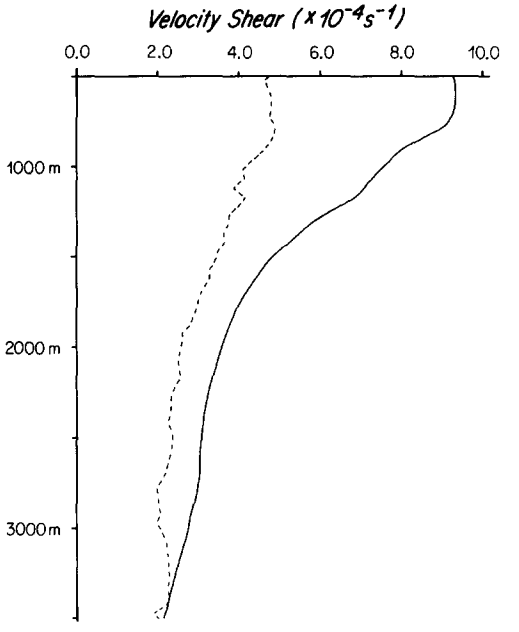

Fig. 6. Velocity shear observed in Drake Passage (solid line) plotted with velocity shear predicted by equation (7) (dashed line).

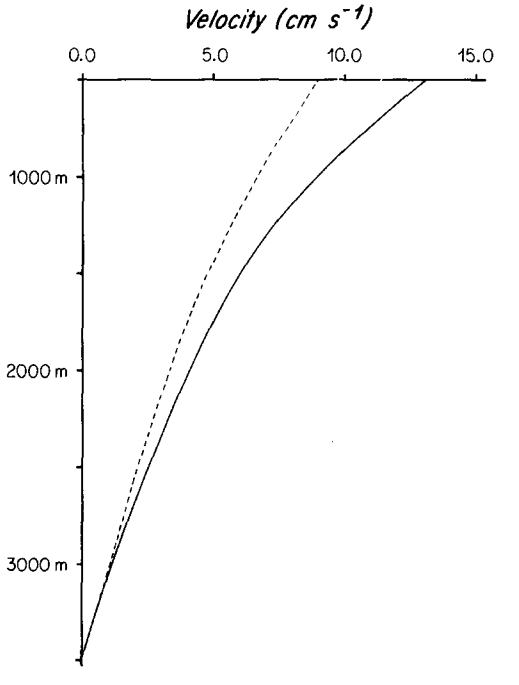

Fig. 7. Velocity referenced to 3500 m as observed in Drake Passage (solid line) vs that predicted by equation (7) (dashed line).

underestimates velocity in the Passage. Again an adjustment in the value of C would improve agreement.

The second test of the model is the transport calculation from the predicted shear profile after equation (8). A width of 590 km is used. If the velocity is assumed zero at 3500 m, the transport predicted is 96 Sv. This number is in reasonable agreement with that cited by NOWLIN and KLINCK (1986) of 134 Sv, which coincidentally is what one gets using the end stations of our hydrographic data referenced to a 3500 m level of no motion. The agreement in transport between model and observation is quite good; halving C would make it remarkable. Taken together with arguments below, it speaks strongly for the applicability of the model to the ACC.

The model successfully predicts the value of baroclinic transport of the ACC. It also incorporates or predicts several observed features of the current. The width of the current, which fills Drake Passage (Fig. 2) and is large all round the pole (Fig. 1), is required by the model since momentum input by the wide band of westerlies over the region (NOWLIN and KLINCK, 1986), must be transferred downward from the surface over the entire circumpolar region. The deep-reaching shear observed in the current (Fig. 2) is necessary for the deep eddy heat fluxes to be large enough to transmit eastward stress downward and for mountain drag to be an effective means of removing eastward momentum. The deflection of the current at mountain ridges (Fig. 1) is certainly an indication of the depth to which the current reaches and may be associated with the mountain drag (MUNK and PALMEN, 1951). Finally, the strong eddy activity in the region (BRYDEN, 1983) and evidence for the role of baroclinic instability processes in providing energy for the eddies (BRYDEN, 1979a) are in accord with the model.

DISCUSSION

While the model incorporates many of the observed features of the ACC, and can only be tested in the Drake Passage where the ACC is well defined and direct eddy heat flux measurements exist, it is important to recognize that it really attempts to describe the large-scale slowly varying baroclinic structure of the current.

MCWILLIAMS *et al.* (1978) found that meridional eddy fluxes of zonal momentum concentrated their model ACC into several narrow jets. Our model assumes that the meridional divergence of the meridional eddy momentum flux is small over the entire width of the ACC. The neglect of this phenomenon in the model may explain the large magnitudes of momentum flux predicted from observations of eddy heat flux by equation (4) (Table 1): while the momentum is transferred to the ocean surface over a large band of latitude by the wind it may be concentrated by these meridional fluxes resulting in larger downward momentum fluxes within the jets, such as the polar frontal zone near which the moorings used are located (NOWLIN and KLINCK, 1986).

While the only direct measurements of eddy heat flux in the ACC are in Drake Passage, KEFFER and HOLLOWAY (1988) apply a turbulence closure scheme to eddy activity measured by a satellite altimeter. They use this to estimate eddy heat flux indirectly. They arrive at a cross-polar front eddy heat flux of 0.7×10^{15} W. Distributing this uniformly over an ocean 4000 m deep and 20,000 km around gives a heat flux of 0.2°C cm s^{-1}, somewhat lower than the average of those cited in Table 1. Using an approximate average vertical stratification of $\overline{\theta}_z = 0.06 \times 10^{-4}$°C cm^{-1} at 59°S, equation (4) gives a downward momentum flux of 4 dyn cm^{-2} with Keffer and Holloway's eddy

heat flux estimate. Once again, this high frontal value may arise from a meridional concentration of zonal momentum input over a wide band by the wind by horizontal eddy momentum flux.

While eddy heat flux in the ACC has only been directly measured in Drake Passage, one might expect eddy statistics in the constricted region of Drake Passage to be anomalous with regard to the current as a whole. An analysis of FGGE drifters in the Southern Ocean by PATTERSON (1985) shows an inhomogeneous distribution of surface eddy kinetic energy in the region. Drake Passage is one of several areas of high surface eddy kinetic energy, most of which are associated with the major ridge systems mentioned here. Measurements in Drake Passage show a local flux of downward momentum larger than that of the wind stress (Table 1). Of course, only the sign and gross magnitude of these statistics is meaningful. What is needed to complement measurements in Drake Passage is a long-term deployment of current meter arrays in the ACC outside of Drake Passage. Such an array would aid in the extrapolation of heat flux measurements from Drake Passage to the whole of the ACC. The data would be useful from the point of view of this study and for the Southern Ocean heat budget (GORDON and OWENS, 1987).

The model is a steady-state one, and as such does not address variability in the current. However, observational and theoretical work has been done on time variability of the ACC. WEARN and BAKER (1980) noted no evidence for strong interannual variability in the baroclinic transport of the ACC. Large fluctuations in the transport of the ACC across the Drake Passage at 500 m measured by Wearn and Baker with time scales of 30 days or more are well correlated with the variations in wind stress integrated over the Southern Ocean, with the former lagging the latter by a period of about 9 days. This rapid rate of adjustment indicates that the transport variation is in the barotropic, not the baroclinic, field. CLARKE (1982) argues analytically that response to wind stress variations of this time scale is barotropic. He finds that only for variations in wind stress on scales of much greater than a few months will there be any variation in the baroclinic transport. Thus we expect that only a long time scale change in wind stress would show up in the baroclinic structure described in the model given here.

Directly measuring bottom pressure drag is difficult. No data exist to measure the pressure gradients across major ridges in the region. These gradients would remove zonal momentum by bottom pressure drag. The problem comes down to the old one of reference level for geostrophic velocity: an absolute pressure field is needed to reference dynamic height across the ridges. Some evidence for bottom pressure drag can be found in the baroclinic field's tendency to deflect around ridges (Fig. 1) but this evidence is incomplete without knowledge of the barotropic field. Deep hydrographic sections across a ridge system (such as the Macquarie Ridge) that obstructs the ACC would be essential to delineate bottom pressure drag. To be useful the velocity field at a deep level would need to be determined just above the peak of the topography with some combination of acoustic doppler velocity data, satellite altimeter measurements, and deep current meters.

Recently the production of topographic form drag by the interaction of large bumps and small seamounts with eddies has been investigated (HOLLOWAY, 1987). This work presents an alternate type of drag to that exerted by large ridges on a mean current as discussed by MUNK and PALMEN (1951). It is not clear which mechanism provides the most effective removal of momentum through form drag. However, this uncertainty does

not effect our model, which focuses on the downward transfer of momentum through the water column. A field experiment as discussed above might yield some insight into this question.

Numerical models of ocean circulation allow for a degree of dynamical analysis that would be prohibitively expensive in time and money if attempted in the real ocean. The Fine Resolution Antarctic Model, or FRAM, should provide a good deal of insight into the dynamics of the ACC (KILLWORTH and ROWE, 1987). The resolution (1/3° N–S and 1/4° E–W) should allow eddies to play a role in the dynamics. Furthermore, the use of the primitive equations and the inclusion of realistic bottom topography and coastline which that allows should shed more light on the role of eddies and bottom topography in the zonal momentum budget of the ACC.

The model presented here is a simple one, but its success in predicting the gross structure and transport of the ACC argues for its basic validity. Of course, it is possible that lateral momentum fluxes may play a part in redistributing the zonal momentum within the circumpolar belt in the upper part of the current as discussed above, and they may also remove some small fraction of zonal momentum from the current. The lessening of eddy heat flux values with depth seen in Table 1 may be real and is in accord with this hypothesis. The observational and numerical work discussed above would aid greatly in expanding our understanding of the circumpolar zonal momentum balance and dynamics proposed here.

Acknowledgements—E. Brady was invaluable in data processing and figure preparation. M. Woodgate-Jones performed initial data processing. M. A. Lucas did the typing. G. Holloway, P. Killworth, M. McCartney, L. Thompson, J. Toole and an anonymous referee all made helpful comments on earlier drafts of the text. This work was done while G.C.J. was an Office of Naval Research Secretary of the Navy Graduate Fellow in the M.I.T.–W.H.O.I. Joint Program. H.L.B. was supported by the National Science Foundation under grant OCE85-4125. WHOI contribution no. 6739.

REFERENCES

BRYDEN H. L. (1979a) Poleward heat flux and conversion of available potential energy in Drake Passage. *Journal of Marine Research*, **37**, 1–22.

BRYDEN H. L. (1979b) Notes on 1977 Drake Passage Cluster array measurements, 11 pp. (unpublished manuscript).

BRYDEN H. L. (1983) The Southern Ocean. In: *Eddies in marine science*, A. L. ROBINSON, editor, Springer-Verlag, Berlin, 609 pp.

BRYDEN H. L. and R. A. HEATH (1985) Energetic eddies at the northern edge of the Antarctic Circumpolar Current in the southwest Pacific. *Progress in Oceanography*, **14**, 65–87.

CLARKE A. J. (1982) The dynamics of large-scale, wind-driven variations in the Antarctic Circumpolar Current. *Journal of Physical Oceanography*, **12**, 1092–1105.

FOSTER T. A. (1972) Current measurements in the Drake Passage. M.S. Thesis, Dalhousie University, Halifax, Nova Scotia, Canada, 61 pp.

GILL A. E. (1968) A linear model of the Antarctic Circumpolar Current. *Journal of Fluid Mechanics*, **32**, 465–488.

GILL A. E. and K. BRYAN (1971) Effects of geometry on the circulation of a three-dimensional southern-hemisphere ocean model. *Deep-Sea Research*, **18**, 685–721.

GORDON A. L. and W. B. OWENS (1987) Polar oceans. *Reviews of Geophysics*, **25**, 227–233.

GORDON A. L., E. MOLINELLI and T. BAKER (1978) Large-scale relative dynamic topography of the Southern Ocean. *Journal of Geophysical Research*, **86**, 3023–3032.

GORDON A. L., E. J. MOLINELLI and T. N. BAKER (1982) *Southern Ocean Atlas*. Columbia University Press, New York, 34 pp. and 248 plates.

GREEN (1970) Transfer properties of the large-scale eddies in the general circulation of the atmosphere. *Quarterly Journal of the Royal Meteorological Society*, **96**, 157–185.

HOLLOWAY G. (1987) Systematic forcing of large-scale geophysical flows by eddy-topography interaction. *Journal of Fluid Mechanics*, **184**, 463–476.

HOSKINS B. J. (1983) Modeling of the transient eddies and their feedback on the mean flow. In: *Large-scale dynamical processes in the atmosphere*, Ch. 7, B. HOSKINS and R. PEARCE, editors, Academic Press, London, pp. 169–199.

KEFFER T. and G. HOLLOWAY (1988) Estimating Southern Ocean eddy flux of heat and salt from satellite altimetry. *Nature*, **332**, 624–626.

KILLWORTH P. D. and M. A. ROWE (1987) FRAM, the Fine Resolution Antarctic Model. *Ocean Modeling*, **74**, 10–11.

MCWILLIAMS J. C., W. R. HOLLAND and J. S. CHOW (1978) A description of numerical Antarctic Circumpolar Currents. *Dynamics of Atmospheres and Oceans*, **2**, 213–291.

MUNK W. H. and E. PALMEN (1951) Note on the dynamics of the Antarctic Circumpolar Current. *Tellus*, **3**, 53–55.

NOWLIN W. D., Jr and J. M. KLINCK (1986) The physics of the Antarctic Circumpolar Current. *Reviews of Geophysics*, **24**, 469–491.

NOWLIN W. D., Jr, T. WHITWORTH III and R. D. PILLSBURY (1977) Structure and transport of the Antarctic Circumpolar Current at Drake Passage from short-term measurements. *Journal of Physical Oceanography*, **7**, 788–802.

PATTERSON S. L. (1985) Surface circulation and kinetic energy distributions in the southern hemisphere oceans from FGGE drifting buoys. *Journal of Physical Oceanography*, **15**, 865–884.

PIOLA A. R., H. A. FIGUEROA and A. A. BIANCHI (1987) Some aspects of the surface circulation south of 20°S revealed by First GARP Global Experiment drifters. *Journal of Geophysical Research*, **92**, 5101–5114.

REID J. L. and W. P. NOWLIN Jr (1971) Transport of water through the Drake Passage. *Deep-Sea Research*, **18**, 51–64.

RHINES P. B. and W. R. HOLLAND (1979) A theoretical discussion of eddy-driven mean flows. *Dynamics of Atmospheres and Oceans*, **3**, 289–325.

STOMMEL H. (1957) A survey of ocean current theory. *Deep-Sea Research*, **4**, 149–184.

STOMMEL H. (1962) An analogy to the Antarctic Circumpolar Current. *Journal of Marine Research*, **20**, 92–96.

STONE P. H. (1972) A simplified radiative-dynamical model for the static stability of rotary atmospheres. *Journal of the Atmospheric Sciences*, **29**, 405–418.

STONE P. H. (1974) The meridional variation of the eddy heat fluxes by baroclinic waves and their parameterization. *Journal of the Atmospheric Sciences*, **31**, 444–456.

WEARN R. B., Jr and D. J. BAKER, Jr (1980) Bottom pressure measurements across the Antarctic Circumpolar Current and their relation to wind. *Deep-Sea Research*, **27**, 875–888.